HAL
open science

Simultaneous meta-modeling for both input and output spaces for rapid design space exploration in structural shape optimization

Balaji Raghavan, Piotr Breitkopf, Pierre Villon

To cite this version:

Balaji Raghavan, Piotr Breitkopf, Pierre Villon. Simultaneous meta-modeling for both input and output spaces for rapid design space exploration in structural shape optimization. 11e colloque national en calcul des structures, CSMA, May 2013, Giens, France. hal-01717026

HAL Id: hal-01717026

https://hal.science/hal-01717026

Submitted on 25 Feb 2018

HAL is a multi-disciplinary open access archive for the deposit and dissemination of scientific research documents, whether they are published or not. The documents may come from teaching and research institutions in France or abroad, or from public or private research centers.

L'archive ouverte pluridisciplinaire **HAL**, est destinée au dépôt et à la diffusion de documents scientifiques de niveau recherche, publiés ou non, émanant des établissements d'enseignement et de recherche français ou étrangers, des laboratoires publics ou privés.

Public Domain

CSMA 2013
11e Colloque National en Calcul des Structures
13-17 Mai 2013

Simultaneous meta-modeling for both input and output spaces for rapid design space exploration in structural shape optimization

Balaji Raghavan[1], Piotr Breitkopf[1], Pierre Villon[1]

[1]Laboratoire Roberval UMR 7337 UTC-CNRS, Universite de Technologie de Compiegne, Labex MS2T

Résumé — Engineering design problems generally involve a high-dimensional input space of design variables yielding an output space by means of costly high-fidelity evaluations. In order to decrease the overall cost, reduced-order models for the output space such as Proper Orthogonal Decomposition (POD) and proper Generalized Decomposition (PGD) are a promising area of research. However, little research has been conducted into alleviating the problems associated with a high-dimensional input space. In this paper, we present a simultaneous meta-modeling protocol for both spaces : reparametrization of the input space by constrained shape interpolation using the α-manifold of admissible shapes (finite element/CFD meshes, etc), and constrained Proper Orthogonal Decomposition for reducing the output space and apply the approach to two industrial shape optimization problems.
Mots clés — Input space reduction, model reduction, design, diffuse approximation.

1 Introduction

When "high fidelity" computer simulations (finite elements, finite volumes, etc.) are used for calculating the objective functions and nonlinear constraints in the process of optimizing mechanical systems, the CPU time frequently becomes disproportionately large. This is due to the cost of individual simulations, the number of simulations or function evaluations needed, and the various additional aspects like license management of the legacy codes and the stability of a complex simulation chain involving multiple codes.

All of these brought about a need for the development and validation of efficient surrogate-based methods in design optimization. Some of the recent advances in surrogate-based design methodology have been thoroughly discussed in [1]. In physical modeling, several techniques have been used to replace a complicated numerical model by a lower-order meta-model, like polynomial response surface methodology (RSM), kriging, least-squares regression and Moving Least Squares [2]. Surrogate functions and reduced-order meta-models have also been used in control systems to reduce the order of the overall transfer function [3]. [4] proposed a goal-oriented, model-constrained optimization framework

A popular physics-based meta-modeling technique consists of carrying out the approximation on the full vector fields using PCA and Galerkin projection [5] in CFD [6] as well as in structural analysis [7]. This approach has been successfully applied to a number of areas such as flow modeling [8, 9] optimal flow control [10], aerodynamics design optimization [11] or structural mechanics [12].

However, this requires manipulation of the input variables $\overline{V}$. Now for complex shapes the dimensionality d can be very high [13] and can greatly exceed the *intrinsic dimensionality* of the design problem. Another far more serious implication is the generation of inadmissible/infeasible structural shapes [14], which could eventually lead to crashes of either the mesh generator or the solver. This was pointed out in [15] where *none* of the POD solutions, and only a few of the constrained POD solutions could be validated, since nearly ALL of the optimal geometries obtained were inadmissible and generated errors in the CAD stage !

A final inconvenience is that gradients/sensitivities need to be calculated using either finite differences or the Adjoint method [16]. All in all, geometric parameterization is an impediment to truly non-intrusive [17] optimization using a clearly separated *offline/online* approach that would allow for interactive design using, for example, a tablet PC.

The phenomenon of CAD failure due to the generation of inadmissible shapes is due to the difficulties

in expressing all the technological and common sense constraints needed to convert a set of geometric parameters to an admissible shape. This issue is frequently encountered but remains relatively under-discussed in the context of design and optimization, and is the motivation for our work. While traditional shape morphing ([18, 19]) is popular, it requires a single reference shape and an arbitrary definition of the morphing boxes and control points.

The authors have not observed much if any research into using decomposition-based surrogate models for reducing dimensionality of the design domain in design or shape optimization [20]. This area is promising considering the obvious advantages of having far fewer parameters describing the domain with **implicit** verification of technological/admissibility constraints : better applicability to gradient-based solvers due to reduced dimensionality, and from the implementation point of view, a separation between the CAD and the optimization phases in system design by giving the optimization group a protocol to re-parameterize structural shapes for a given set of admissible shapes/meshes that can be generated by the CAD group, and using the presented algorithm (or a variant thereof) on these to get the new set of design variables.

In this paper, we develop an approach that builds up a design space by *learning* using *shape interpolation* between shape/mesh instances given by a sequence of parameter values. The input space is reduced using first direct POD on a set of *admissible* structural shapes in the *local neighborhood* of the evaluation point, followed by analyzing the *inter-relationship* between the α's in this local neighborhood ($\mu(\bar{\alpha}) = 0$: the manifold of α's), represented using a local parametric expression $\bar{\alpha} = \bar{\alpha}(\bar{t})$. The output space (physics) is modeled using constrained Proper Orthogonal Decomposition [21] giving the smallest set of coefficients $\beta_1 ... \beta_m$ needed to conserve *linear* objective and constraint functions. The POD coefficients for the shape *and* physics are then analyzed *together* to get the local parametric expression for both α's as well as β's in the neighborhood of the evaluation point.

In addition, our approach gives an elegant, practical and straightforward method to compute the so-called "shape derivatives" of the performance objective(s), which are increasingly popular as used in "shape calculus" [22, 23, 24, 25].

The methodology and the overall algorithm are described in the next section with the help of a simple structural test case, and then applied to an industrial shape optimization problem in section 3 with a full set of numerical results and discussion before the concluding paragraph.

2 Simultaneous meta-modeling using "shape space" and constrained POD

The key points of our approach in this paper are as follows :

1. We build the parameterization scheme (shape space) ”learning” directly from example admissible **shapes**.
2. We perform POD directly on the structural shapes in a*local neighborhood* of 7-10 admissible shapes.
3. We do *not* truncate the basis, i.e. we retain ALL the modes without losing precision. Instead we look at the inter-relationship between the projection coefficients.
4. We calculate gradients, etc in this *local shape space* to get the shape derivatives of the performance objectives.

To this end, consider a typical structural optimization problem in equation 1 with geometric dimensionality d where we would like to minimize the performance objective $J(\bar{V})$ (calculated using FEM) :

$$\begin{aligned} \text{Find } \bar{V}_{opt} = \underset{\bar{V} \in [\bar{V}_{min}, \bar{V}_{max}] \subset \mathcal{R}^d}{Argmin} \quad & J(\bar{U}(\bar{V})) \\ \text{such that } \mathbf{K}(\bar{V})\bar{U}(\bar{V}) = \bar{F} & \text{(equation of equilibrium)} \\ \text{and } \bar{C}(\bar{V}) = \bar{0} & \text{(shape/admissibility constraint)} \\ \text{and } A^H(\bar{V}) \geq A_o & \text{(mass constraint)} \end{aligned} \tag{1}$$

where $\mathbf{K}(\bar{V})$ (stiffness matrix), $\bar{U} = \mathbf{K}^{-1}\bar{F}$, force $\bar{F}$ and A_o are constants, $\bar{C} : [\bar{V}_{min}, \bar{V}_{max}] \rightarrow \mathcal{R}^{n_c}$ is the shape constraint function that is unknown/difficult to express analytically (n_c =size of constraint vector)

where $\forall \bar{V} \in \mathcal{E}_e \subset [\bar{V}_{min}, \bar{V}_{max}], \bar{C}(\bar{V}) = \bar{0}$, $\mathcal{E}_e$ is the subset of admissible shapes.
So we need to *implicitly* satisfy the admissibility criterion i.e. $\bar{V}(\bar{\alpha}) \in \mathcal{E}_e$ reducing (1) to :

$$\text{Find } \bar{\alpha}_{opt} = \underset{\Phi=const}{Argmin}\{J(\bar{\alpha}, \Phi)\},$$
$$\text{s.t. } \bar{\alpha} \in [\bar{\alpha}_{min}, \bar{\alpha}_{max}] \subset \mathcal{R}^m, c(\bar{\alpha}) = 0, a^h(\bar{\alpha}) \leq 0, \tag{2}$$

where $m << d$. The basis Φ is fixed in (2) since even though it will vary globally, (2) is applied locally.

2.1 Design domain and shape indicator functions

We first study the range of admissible shapes (i.e. snapshots [34]) sweeping the neighborhood of the evaluation point in the physical design domain, typically in a Lagrangian description with a sampling of the geometry-based design variables within their range $\bar{V} \in [\bar{V}_{min}, \bar{V}_{max}] \subset \mathcal{R}^d$, for an initial random sampling of M **admissible** designs $\bar{V}^1..\bar{V}^M$ (i.e. satisfying $\bar{C}(\bar{V}) = 0$) and convert to the corresponding shape indicator functions $S^1...S^M$. here *voxelization* has been used.

2.2 Principal Components Analysis

This is the first stage of the model reduction. We calculate the deviation and covariance matrices D_s and C_v for the snapshots $S^1..S^M$:

$$D_s = \left[\begin{array}{cccc} S^1 - \bar{S} & S^2 - \bar{S} & \ldots & S^M - \bar{S} \end{array} \right] \text{ and } C_v = D_S.D_S^T \tag{3}$$

allowing us to express any S^j in terms of the eigenvectors $\bar{\phi}_i$ of C_v where $M << N_c$ = number of snapshots, S^i = i^{th} individual snapshot and $\bar{S}$ is the mean snapshot.

$$S^j = \bar{S} + \sum_{i=1}^{M} \alpha_{ij} \bar{\phi}_i \text{ , } \alpha_{ij} = \bar{\phi}_i^T S^j \tag{4}$$

for the jth indicator function. (NOTE : $-1 \leq \bar{\phi}_i \leq 1$, $0 \leq \bar{S} \leq 1$ while S^j is binary). The usual reduction approach would be to limit the basis to the first $m << M$ most "energetic" modes :

$$\tilde{S}^j = \bar{S} + \sum_{i=1}^{m} \alpha_{ij} \bar{\phi}_i \text{ and } \varepsilon(m) = 1 - \frac{\sum_{i=1}^{m} \lambda_i}{\sum_{i=1}^{M} \lambda_i} \tag{5}$$

where $\varepsilon(m)$ is the relative projection error, λ's are the eigenvalues of C_v. However, the last equation does not provide a sufficient basis for establishing the value of m since we need to specify a threshold value for ε.

2.3 Model reduction by constructing the local α-manifold

Since the α's can not be directly interpreted as new design variables without taking into account the possible inter-relationships that exist between them so as to render feasible shapes. In addition, truncating the basis Φ would limit precision. Therefore, instead of truncating the basis, we instead analyze the inter-relationships between these α's obtained from the M snapshots in order to detect the true dimensionality (p) of the design domain.
In the general case, we obtain a p-dimensional manifold with the local parametric expression $\bar{\alpha} = \bar{\alpha}(\bar{t}), \bar{t} \in R^p, p \leq d$). $t_1....t_p$ are local parameters that allow us to move along the tangent plane to the manifold. For e.g., from the previous section - for a plate with an elliptical hole of varying radii, the α's form a set of two-dimensional manifolds (figure **??**) rather than a cloud of points in 3D space *regardless of the particular triplet of modes used*, clearly indicating that the design domain is parametrized by **two** local parameters t_1, t_2. This means that $\alpha_1 = \alpha_1(t_1, t_2), \alpha_2 = \alpha_2(t_1, t_2)....$
Basically, points lying outside the manifolds always produce inadmissible shapes so the surfaces $\alpha_1, \alpha_2, \ldots$ vs $t_1, t_2 ... t_p$ may be interpreted as the set of all possible "constraints" (direct geometric constraints, technological constraints etc that are difficult to express mathematically) on the geometric parameters $\bar{V}$ in the α-space. In other words, **the α-manifold represents the feasible region of admissible shapes**. In our work, we

introduce this local parametric expression $\bar{\alpha} = \bar{\alpha}(t_1, ..., t_p))$ using Diffuse Approximation [30]. Consider the snapshots in α-space : $\bar{\alpha}^1, ...\bar{\alpha}^M \in \mathcal{R}^M$. We would like to implement an algorithm that :
1. Detects the "true"/inherent dimensionality of the design domain ($p \leq M$) from the local rank of the α-manifold in the vicinity of the evaluation point, so that the feasible region may (locally) be expressed as $\alpha_1 = \alpha_1(t_1..t_p), ...\alpha_M = \alpha_M(t_1..t_p)$.
2. Constrains the evaluation point ($\bar{\alpha}^{ev}$) to stay on the feasible region of admissible shapes, during the course of the optimization.

To locally detect the dimensionality of the $\alpha_1...\alpha_M$ hyper-surface in the neighborhood of $\bar{\alpha}^{ev}$, we extend the method of Fukunaga and Olsen [35]. First, we establish a sufficiently dense local neighborhood. Let $\bar{\beta}_1...\bar{\beta}_{nbd}$ be *nbd* neighboring points in α-space, we next use a polynomial basis centered on $\bar{\alpha}^{ev}$

$$\mathbf{P}(\bar{\alpha}_{ev}) = \begin{bmatrix} 1 & \beta_1^1 - \alpha_1^{ev} & \beta_2^1 - \alpha_2^{ev} & .... & \beta_M^1 - \alpha_M^{ev} & .... \\ . & . & . & .... & . & .... \\ 1 & \beta_1^{nbd} - \alpha_1^{ev} & \beta_2^{nbd} - \alpha_2^{ev} & .... & \beta_M^{nbd} - \alpha_M^{ev} & .... \end{bmatrix} \tag{6}$$

with an appropriate weighting function (e.g. Gaussian $w(d) = e^{-cd^2}$) and assemble the moment matrix $M_t = P^T W P$, where W is the diagonal matrix whose elements correspond to the weighted contributions of the nodes $\bar{\beta}_1...\bar{\beta}_{nbd}$. Next, we detect the local rank of the manifold by calculating the rank of the moment matrix from the number of singular values of M_t, this gives us the dimensionality $p \leq M$.

2.4 Diffuse predictor-corrector "walking" algorithm

This algorithm will bring the design point (in α-space) in the optimization algorithm (or interactive design procedure) back down to the α-manifold in subsequent iterations using a predictor-corrector scheme consisting of the following steps (figure **??**).
1. Let Q_i be the current design point : $\bar{\alpha}_{ev}$ in α-space. In the predictor stage, using a single Quasi-Newton step from Q_i, let Q_{i+1}^0 be the new candidate point that needs to be brought back on to the manifold/feasible region (correction phase). We first establish the α-neighborhood $\bar{\mu}_1...\bar{\mu}_{nbd}$ of Q_{i+1}^0.
2. Calculate the centroid $\bar{\mu}_m = (\sum_{i=1}^{nbd} \bar{\beta}_i)/nbd$.
3. Find the centroidal plane for the neighborhood from the eigenvectors of the covariance matrix C_{nbd}, the first eigenvector representing the plane normal :

$$C_{nbd} = (1/nbd) \sum_{i=1}^{nbd} (\bar{\mu}_i - \bar{\mu}_m)(\bar{\mu}_i - \bar{\mu}_m)^T \ , \ (\bar{v}_1, \bar{v}_2...) = eigenvectors(C_{nbd}) \tag{7}$$

4. Project the evaluation point as well as the neighborhood points in the local coordinate system $\bar{v}_1, \bar{v}_2...$ (origin at centroid $\bar{\beta}_m$) to get the local co-ordinates $h, t_1...t_p$ for a general $\bar{\alpha}$ where h is height over the centroidal plane using :

$$h = \bar{v}_1^T (\bar{\alpha} - \bar{\mu}_m) \ , \ t_1 = \bar{v}_2^T \bar{\alpha} \ , \ etc \tag{8}$$

5. We next obtain the shape (indicator function) and calculate J for the evaluation point. We recreate the structural shape for an arbitrary design point ($\bar{t}$) using the α coefficients obtained from $\bar{t}$ (location on the α-manifold), and thus the indicator function $\tilde{S}$:

$$\tilde{S}(\bar{t}) = \bar{S} + \sum_{i=1}^{m} \alpha_i(\bar{t}) \bar{\phi}_i \tag{9}$$

To calculate the objective function $J(\tilde{S})$ using a response surface between the output-space and input space meta-models giving us the output space POD coefficients $\beta_1..\beta_m$ as $\bar{\beta}(\bar{\alpha}(\bar{t}))$. We now get the objective function using $J(\tilde{v})$ where $\tilde{v}$ is the physical vector field reduced by the physics meta-model.

$$J \approx J(\tilde{v}) = J(\bar{v}_0 + \Psi \bar{\beta}(\bar{\alpha}(\bar{t}))) \tag{10}$$

6. Do the Diffuse Approximation for $\bar{\alpha}^{ev}$ as well as the objective function J using the *nbd* neighboring points to get the local surface $h = \tilde{h}(t_1...t_p)$ using a polynomial basis $\mathbf{P_q}(\bar{\alpha}^{ev})$ with weighting $\mathbf{W}$, and

$J = \tilde{J}(t_1..t_p)$ in a similar fashion using a basis $\mathbf{P_j}(\bar{\alpha}^{ev})$.

$$[\tilde{h}(\bar{t}^{ev}), \frac{\partial \tilde{h}}{\partial t_1}(\bar{t}^{ev}), \frac{\partial \tilde{h}}{\partial t_2}(\bar{t}^{ev}), ...]^T = (\mathbf{P_q}^T \mathbf{W} \mathbf{P_q})^{-1} \mathbf{P_q}^T \mathbf{W} [h_1, ..., h_{nbd}]^T \tag{11}$$

$$[\tilde{J}(\bar{t}^{ev}), \frac{\partial \tilde{J}}{\partial t_1}(\bar{t}^{ev}), \frac{\partial \tilde{J}}{\partial t_2}(\bar{t}^{ev}), ...]^T = (\mathbf{P_j}^T \mathbf{W} \mathbf{P_j})^{-1} \mathbf{P_j}^T \mathbf{W} [J_1, ..., J_{nbd}]^T \tag{12}$$

where the term in the LHS is the local tangent hyper-plane at Q_0 in the neighborhood $\bar{\beta}^1 ... \bar{\beta}^{nbd}$.
7. We then project the point Q^0_{i+1} onto this tangent plane to get the adjusted evaluation point Q^1_{i+1}, and then repeat by finding the new neighborhood, tangent plane and projection point ,etc till the evaluation point stops changing Q^f_{i+1}.

2.5 Gradient and Hessian : Diffuse "Shape derivatives"

Our concept of shape derivatives ∇J (and Hessian H with additional derivatives) is simply that of the ”diffuse” derivatives [30] of J with respect to $\bar{t}$ (from the previous section), since $\bar{t}$ is simply the *local description* of the shape manifold :

$$\nabla J = [\frac{\partial \tilde{J}(\bar{t})}{\partial t_1}, \frac{\partial \tilde{J}(\bar{t})}{\partial t_2}, ..] = \Phi^T \frac{dJ}{dS} \tag{13}$$

which is simply the *projection* of the *Eulerian derivative* onto Φ.

2.6 Optimization in shape-space

The optimization problem in reduced-space now becomes :

$$\begin{aligned} \text{Find } \bar{t}_{opt} &= Argmin_{\bar{t} \in \mathcal{R}^p} \{J(\bar{\alpha}(\bar{t}))\} \\ \text{s.t. } c(\bar{\alpha}(\bar{t})) = 0, a^h(\bar{\alpha}(\bar{t})) &\leq 0, \bar{\alpha}_{min} \leq \bar{\alpha}(\bar{t}) \leq \bar{\alpha}_{max} \end{aligned} \tag{14}$$

where c represents the admissibility constraint (i.e. the α-manifold), a^h represents the mass constraint, and $\bar{\alpha}_{min}$ and $\bar{\alpha}_{max}$ are the bounds on $\bar{\alpha}$.

3 TEST-CASE : Optimization of engine intake port

3.1 Description of Test-Case : Intake geometry and CAD issues

This test-case is related to the performance optimization of an engine intake (figure 1(a) and (b)), originally proposed by Renault as a third benchmark optimization case for the OMD2 project [36]. The intake pipe and port system has a very complex structural shape with physical details as shown in figure 1(c). We optimize two important performance objectives : the mass flow rate Q through the cylinder and tumble pattern of flow (vorticity τ). This variable 3D geometry is parameterized by using 93 bounded

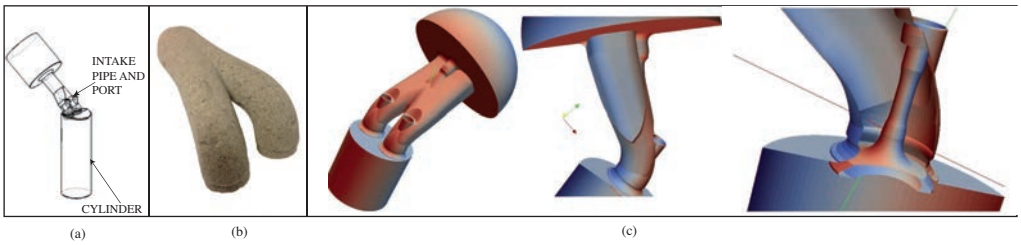

Fig. 1 – (a) Full system (b) Sand model of intake pipe (c) External & internal details of engine intake

geometric design variables $\bar{V} \in [\bar{V}_L, \bar{V}_U] \subset \mathcal{R}^{93}$ in CATIA with CAD failure rate of over **60%**.

3.2 Results & Discussion

3.2.1 α-manifolds for the engine intake

The α-manifolds for the design problem of an engine intake are shown in figures 2 indicating a dimensionality p **less than** 3, and this has been drawn using a set of snapshots corresponding to the set of admissible shapes generated using 93 geometric parameters.

This is verified using the Fukunaga-Olsen algorithm [35] in figure 3(a). A $p = 1$ approximation would

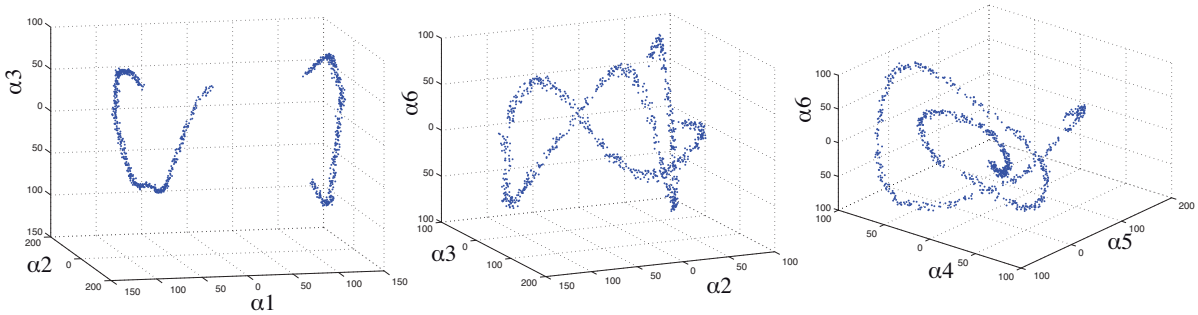

Fig. 2 – α-manifolds for the engine intake problem

be particularly attractive (figure 3(b)).

It bears mentioning that the analysis of dimensionality from a cloud of points in ND-space is a multi-

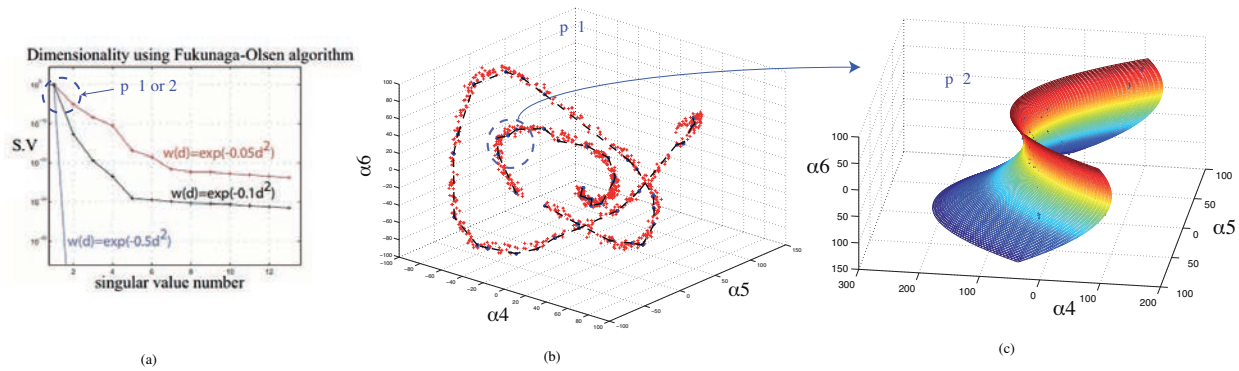

Fig. 3 – (a) Dimensionality p calculation, (b) Constrained shape interpolation using $p = 1$, (c) α-manifold approximation using $p = 2$

scale problem, so when resampled in a smaller neighborhood, p **might** creep up to a value of 2 as illustrated in figure 3(c) showing the 2D α-manifolds for the same problem.

3.2.2 Single-parameter shape morphing for 93-parameter engine intake

Keeping the previous discussion in mind, we can safely build a single parameter ($p = 1$) approximation/representation of the engine intake design space. So from the set of α-manifolds, we generate a set of 58 points on the axis of the manifold, yet again using the Diffuse Approximation [30]. These are shown in figure 3(b). We can now reconstruct the 58 admissible shapes using CATIA to generate smooth transitions in structural shape i.e. vary 93 geometric parameters using a single parameter (position along the axis of the manifold), giving us $\bar{V} = \bar{V}(\alpha_1(t), \alpha_2(t) \ldots \alpha_M(t))$, while constantly staying in the feasible region. This will greatly simplify the task of optimizing the intake shape i.e. $\bar{V}_{opt}$ for a given objective.

3.2.3 Design space exploration using 2 parameters and interactive design using meta-models

Figure 4 shows 4 frames of the interactive design for the engine intake problem, using 2D α-manifolds in MATLAB for 4 different locations on shape space, easily handled using modest resources.

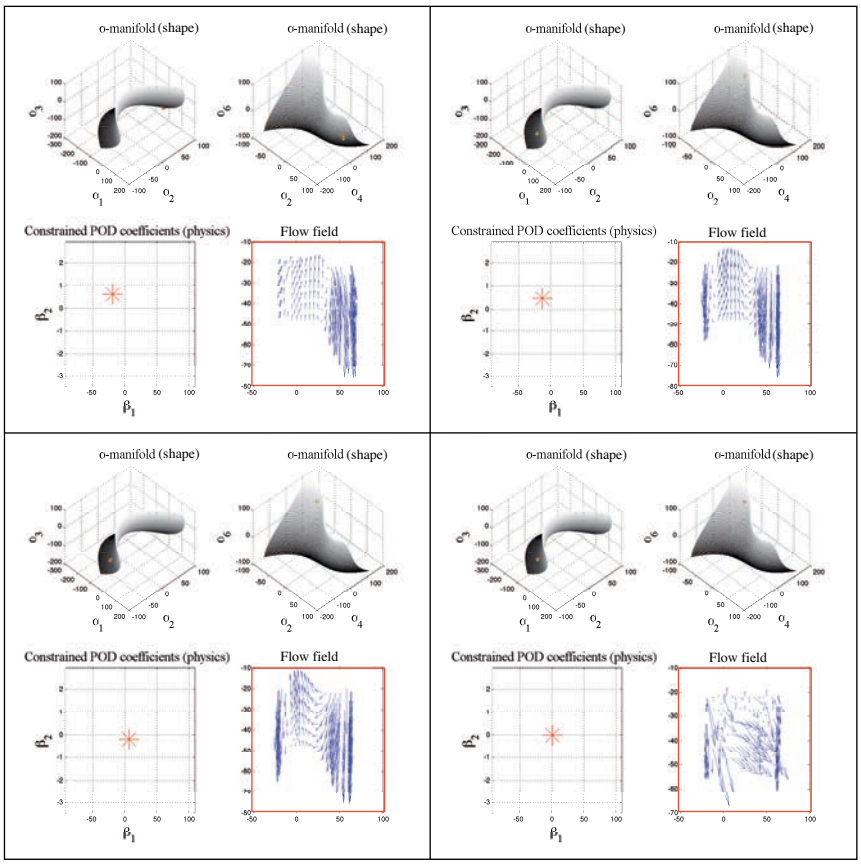

Fig. 4 – Interactive design using α-manifolds and CPOD coefficients for the 6-parameter intake problem

4 Références bibliographiques

Références

[1] A. I. J. Forrester and A. J. Keane, “Recent advances in surrogate-based optimization.,” *Progress in Aerospace Sciences*, vol. 45, pp. 50–79, 2009.

[2] P. Breitkopf, H. Naceur, A. Rassineux, and P. Villon, “Moving least squares response surface approximation : Formulation and metal forming applications,” *Computers and Structures*, vol. 83, no. 17-18, pp. 1411–1428, 2005.

[3] K. Willcox and J. Peraire, “Balanced model reduction via the proper orthogonal decomposition,” *AIAA Journal*, vol. 40, no. 11, pp. 2323–2330, 2002.

[4] T. Bui-Thanh, K. Willcox, O. Ghattas, and B. van Bloemen Waanders, “Goal-oriented, model-constrained optimization for reduction of large-scale systems,” *Journal of Computational Physics*, vol. 224, no. 2, pp. 880 – 896, 2007.

[5] G. Berkooz, P. Holmes, and J. L. Lumley, “The proper orthogonal decomposition in the analysis of turbulent flows,” *Annu Rev Fluid Mech*, vol. 25, no. 1, pp. 539–575, 1993.

[6] C. Audouze, F. De Vuyst, and P. Nair, “Reduced-order modeling of parameterized pdes using time-space-parameter principal component analysis,” *International Journal of Numerical Methods in Engineering*, vol. 80, no. 8, pp. 1025 – 1057, 2009.

[7] L. Cordier, B. A. El Majd, and J. Favier, “Calibration of pod reduced order models using tikhonov regularization,” *International Journal for Numerical Methods in Fluids*, vol. 63, no. 2, pp. 269–296, 2010.

[8] R. A. Sahan, H. Gunes, and A. Liakopoulos, “A modeling approach to transitional channel flow,” *Computers and Fluids*, vol. 27, no. 1, pp. 121–136, 1998.

[9] M. Couplet, C. Basdevant, and P. Sagaut, “Calibrated reduced-order pod-galerkin system for fluid flow modeling,” *Journal of Computational Physics*, vol. 207, no. 1, pp. 192–220, 2005.

[10] S. S. Ravindran, “A reduced-order approach for optimal control of fluids using proper orthogonal decomposition,” *International Journal for Numerical Methods in Fluids*, vol. 34, no. 5, pp. 425–448, 2000.

[11] P. A. LeGresley and J. J. Alonso, “Airfoil design optimization using reduced order models based on proper orthogonal decomposition,” *Fluids 2000 Conference and Exhibit,Denver, CO*, 2000.

[12] J.-L. Dulong, F. Druesne, and P. Villon, “A model reduction approach for real-time part deformation with nonlinear mechanical behavior,” *International Journal on Interactive Design and Manufacturing*, vol. 1, no. 4, pp. 229–238, 2007.

[13] W.-H. Zhang, P. Beckers, and C. Fleury, “Unified parametric design approach to structural shape optimization,” *International Journal for Numerical Methods in Engineering*, vol. 38, no. 13, pp. 2283–2292, 1995.

[14] A. Veiz and M. Egerland, “Cad-parametric optimization with optislang-ansys workbench,” *4th Weimar optimization and stochastic days*, 2007.

[15] B. Raghavan, M. Hamdaoui, M. Xiao, P. Breitkopf, and P. Villon, “A bi-level meta-modeling approach for structural optimization using modified pod bases and diffuse approximation,” *Computers & Structures*, 2012.

[16] F. Van Keulen, R. Haftka, and N. Kim, “Review of options for structural design sensitivity analysis. part 1 : Linear systems,” *Computer Methods in Applied Mechanics and Engineering*, vol. 194, no. 30-33, pp. 3213–3243, 2006.

[17] R. F. Coelho, P. Breitkopf, and C. Knopf-Lenoir, “Bi-level model reduction for coupled problems,” *Int J Struc Multidisc Optim*, vol. 39, no. 4, pp. 401–418, 2009.

[18] A. Y. N. Sofia, S. A. Meguid, and K. T. Tan, “Shape morphing of aircraft wing : Status and challenges,” *Materials & Design*, vol. 31, no. 3, pp. 1284–1292, 2010.

[19] R. Duvigneau, “Adaptive parameterization using free-form deformation,” *INRIA Research Report RR-5949*, July 2006.

[20] D. Wang and W. Zhang, “A bispace parameterization method for shape optimization of thin-walled curved shell structures with openings,” *International Journal for Numerical Methods in Engineering*, vol. 90, no. 13, pp. 1598–1617, 2012.

[21] M. Xiao, P. Breitkopf, R. F. Coelho, C. Knopf-Lenoir, M. Sidorkiewicz, and P. Villon, “Model reduction by cpod and kriging,” *Int J Struc Multidisc Optim*, vol. 41, no. 4, pp. 555–574, 2009.

[22] S. Jan and J.-P. Zolesio, “Introduction to shape optimization : Shape sensitivity analysis, springer verlag berlin,” 1992.

[23] G. Allaire, F. Jouve, and A.-M. Toader, “Structural optimization using sensitivity analysis and a level-set method,” *Journal of Computational Physics*, vol. 194, no. 1, pp. 363–393, 2004.

[24] F. Murat and J. Simon, “Sur le controle par un domaine geometrique,” *Pre-publication du Laboratoire d’Analyse Numerique, no 76015, Universite de Paris*, vol. 6, 1976.

[25] V. Schulz, “A riemannian view on shape optimization,” *Foundations of Computational Mathematics*, 2012.

[26] L. P. Swiler and G. D. Wyss, “A user’s guide to sandia’s latin hypercube sampling software : Lhs unix library standalone version,” *Sandia National Laboratories*, 2009.

[27] C. Ghnatios, F. Chinesta, and E. Cueto, “Optimizing composites forming processes by applying the proper generalized decomposition,” *International Conference on Advances in Materials and Processing Technologies,Ctr Arts & Metiers ParisTech, Paris, FRANCE*, 2010.

[28] R. F. Coelho, J. lebon, and P. Bouillard, “Hierarchical stochastic metamodels based on moving least squares and polynomial chaos expansion : Application to the multiobjective reliability-based optimization of space truss structures,” *Int J Struc Multidisc Optim*, vol. 43, no. 5, pp. 707–729, 2011.

[29] D. Amsallem, J. Cortial, K. Carlberg, and C. Farhat, “A method for interpolating on manifolds structural dynamics reduced-order models,” *International Journal for Numerical Methods in Engineering*, vol. 80, no. 9, pp. 1241–1258, 2009.

[30] B. Nayroles, G. Touzot, and P. Villon, “Generalizing the finite element method : diffuse approximation and diffuse elements,” *Computational Mechanics*, vol. 10, no. 5, pp. 307–318, 1992.

[31] N. H. Kim and Y. Chang, “Eulerian shape design sensitivity analysis and optimization with a fixed grid,” *Computer Methods in Applied Mechanics and Engineering*, vol. 194, no. 0, pp. 3291–3314, 2005.

[32] A. Kaufman, D. Cohen, and R. Yagel, “Volume graphics,” *IEEE Computer*, vol. 26, no. 7, pp. 51–64, 1993.

[33] S. Oshier and J. A. Sethian, “Fronts propagating with curvature-dependent speed : Algorithms based on hamilton-jacobi formulations,” *Journal of Computational Physics*, vol. 79, pp. 12–49, 1988.

[34] A. Chatterjee, “An introduction to the proper orthogonal decomposition,” *Current Science, Special Section : Computational Science*, vol. 78, no. 7, pp. 808–817, 2005.

[35] K. Fukunaga and D. Olsen, “An algorithm for finding intrinsic dimensionality of data,” *IEEE Transactions on Computers*, vol. 20, pp. 176–183, 1971.

[36] O. project home page, “Last accessed feb 22, 2011,” *http ://omd2.scilab.org/*, 2009.